On the topographic targeting of basal vomeronasal axons through Slit-mediated chemorepulsion

Bernd Knöll, Hannes Schmidt, William Andrews, Sarah Guthrie, Adrian Pini, Vasi Sundaresan and Uwe Drescher*

MRC Centre for Developmental Neurobiology, King's College London, New Hunt's House, Guy's Hospital Campus, London SE1 1UL, UK

*Author for correspondence (e-mail: uwe.drescher@kcl.ac.uk)

Accepted 14 July 2003

Development 130, 5073-5082

doi:10.1242/dev.00726

Summary

The vomeronasal projection conveys information provided by pheromones and detected by neurones in the vomeronasal organ (VNO) to the accessory olfactory bulb (AOB) and thence to other regions of the brain such as the amygdala. The VNO-AOB projection is topographically organised such that axons from apical and basal parts of the VNO terminate in the anterior and posterior AOB respectively.

We provide evidence that the Slit family of axon guidance molecules and their Robo receptors contribute to the topographic targeting of basal vomeronasal axons. Robo receptor expression is confined largely to basal VNO axons, while Slits are differentially expressed in the AOB with a higher concentration in the anterior part, which basal axons do not invade.

Immunohistochemistry using a Robo-specific antibody reveals a zone-specific targeting of VNO axons in the AOB well before cell bodies of these neurones in the VNO acquire their final zonal position. In vitro assays show that Slit1-Slit3 chemorepel VNO axons, suggesting that basal axons are guided to the posterior AOB due to chemorepulsive activity of Slits in the anterior AOB.

These data in combination with recently obtained other data suggest a model for the topographic targeting in the vomeronasal projection where ephrin-As and neuropilins guide apical VNO axons, while Robo/Slit interactions are important components in the targeting of basal VNO axons.

Key words: Robo, Slit, Axon guidance, VNO, Vomeronasal, AOB, Chemorepulsion, Topographic, Olfactory, Pheromone, Mouse

Introduction

Most terrestrial vertebrates have evolved an anatomically and functionally distinct structure, the accessory olfactory or vomeronasal system, which modulates pre-programmed behavioural patterns such as mating and aggression via the detection of pheromones (Del Punta et al., 2002a; Dulac, 2000; Keverne, 2002; Leypold et al., 2002; Mombaerts, 1999; Rodriguez et al., 2000; Stowers et al., 2002). The vomeronasal organ (VNO) is positioned ventrally in the nasal cavity and is the chemosensory apparatus for pheromone detection. VNO axons connect the sensory epithelium of the VNO to the accessory olfactory bulb (AOB), the first relay station in the brain, which is located in a dorsoposterior position on top of the main olfactory bulb (MOB). Secondary projections link the AOB to nuclei in the hypothalamus and amygdala for further information processing (Keverne, 1999).

The axonal projection between the VNO and the AOB is zonally organised. Sensory neurones in the apical zone of the VNO project their axons to the anterior half of the AOB, while the posterior AOB is innervated by axons of the basal VNO (see Fig. 7). This topography was revealed in expression studies on several molecular markers, including vomeronasal receptors, the putative pheromone receptors and Gα-proteins (Dulac and Axel, 1995; Herrada and Dulac, 1997; Jia and Halpern, 1996; Matsunami and Buck, 1997; Ryba and Tirindelli, 1997). Co-expression of the marker proteins tau-*lacZ* and tau-GFP with selected vomeronasal receptors led, for the first time, to the visualisation of a vomeronasal map (Belluscio et al., 1999; Del Punta et al., 2002b; Rodriguez et al., 1999), demonstrating that axons which express the same vomeronasal receptor terminate within the AOB in a specific pattern of spatially conserved groups of glomeruli. Genetic ablation of vomeronasal receptors disrupts this glomerular convergence, and so vomeronasal receptors might act as bifunctional molecules, working both to transduce signals from pheromones and to guide VNO axons. In such mutants, however, vomeronasal axons still project mostly to the appropriate half in the AOB suggesting that other guidance cues must be involved in establishing the integrity of the zone-to-zone projection (Belluscio et al., 1999; Rodriguez et al., 1999). Indeed, two families of axonal guidance molecules, the ephrins and the semaphorins, were recently reported to be involved in the zonal projection of apical vomeronasal axons (Cloutier et al., 2000; Knöll et al., 2001; Walz et al., 2002).

First, ephrin A5 was found to be expressed more strongly on apical than basal VNO axons, while the Epha6 receptor was preferentially expressed in the anterior AOB (Knöll et al., 2001). Thus axons with higher levels of ephrin A proteins project onto a region of the AOB with higher Epha expression (see Fig. 7). This led to a model in which the projection of

apical axons to the anterior AOB is mediated by an attractive guidance mechanism in which ephrin A proteins function as receptors and Epha receptors as ligands. This idea was supported by data from in vitro stripe assays, and also by the analysis of ephrin A5 mutant mice, in which apical axons terminated in both the anterior and (topographically inappropriate) posterior AOB (Knöll and Drescher, 2002; Knöll et al., 2001). Secondly, neuropilin 2, which is part of the receptor complex for some class 3 semaphorins, is expressed on apical but not basal VNO axons. The analysis of neuropilin 2 mutant mice also showed a disruption of the zonal projection of apical VNO axons (Cloutier et al., 2000; Walz et al., 2002). It therefore appears that both ephrin A proteins and neuropilins are involved in the topographic targeting of apical VNO axons to the anterior AOB.

This raises the question of which guidance cues are involved in guiding basal axons to the posterior AOB, as the zonal projection of basal axons (e.g. in neuropilin 2 mutant mice) is normal (Cloutier et al., 2000; Walz et al., 2002).

We present data that indicate that the Slit and Robo axon guidance molecules are candidates to fulfil this function. Robo proteins were first shown to regulate axon crossing at the *Drosophila* midline because of repulsive interactions with Slits secreted from midline cells (Brose and Tessier-Lavigne, 2000; Guthrie, 2001; Nguyen-Ba-Charvet and Chedotal, 2002; Schimmelpfeng et al., 2001; Tear, 1999). Although ipsilaterally projecting axons express Robo constitutively and do not cross the midline, commissural axons are initially Robo negative, which allows them to cross. Robo expression is only evident on axons once they have crossed the midline and so prevents them from re-crossing. In *Drosophila*, the differential expression of Robo is controlled by commissureless (Georgiou and Tear, 2002; Keleman et al., 2002; Kidd et al., 1998a; Kidd et al., 1998b; Myat et al., 2002; Tear et al., 1996).

In vertebrates, three Robo proteins (Robo1, Robo2 and Rig1) and three Slits (Slit1-Slit3) have been identified (Brose et al., 1999; Fricke et al., 2001; Holmes et al., 1998; Itoh et al., 1998; Li et al., 1999; Marillat et al., 2002; Sundaresan et al., 1998; Yuan et al., 1999a; Yuan et al., 1999b). Besides an involvement in midline crossing (Bagri et al., 2002; Hutson and Chien, 2002; Plump et al., 2002), Robo and Slit proteins have been implicated in the pathfinding – but not topographic targeting – of olfactory, retinal, hippocampal and cranial motor axons by exerting a repulsive action (Brose et al., 1999; Erskine et al., 2000; Hutson and Chien, 2002; Li et al., 1999; Nguyen Ba-Charvet et al., 1999; Niclou et al., 2000; Ringstedt et al., 2000).

Materials and methods

Animals

C57/Bl6 mice were used for expression studies and in vitro experiments. The day of the vaginal plug was taken as embryonic day (E) 0.5, and the day of birth as postnatal day 1 (P1).

In situ hybridisation

All in situ hybridisation experiments were performed as previously described (Knöll et al., 2001). The cRNAs probes to rat *Robo1*, *Robo2* and rat *Slit1-Slit3* (Brose et al., 1999) were kindly provided by Dr Marc Tessier-Lavigne (Stanford University, Stanford, CA).

Expression analysis of Slits

For detection of Slits on sections of the accessory olfactory bulb, we used the protocol of Conover et al. (Conover et al., 2000). In brief, P1 embryos were fixed in ice-cold 4% paraformaldehyde (PFA) for 3-5 hours, embedded in 5% low-melting agarose and vibratome-sectioned at 100-150 μm. After blocking with 10% newborn goat serum (NGS)/2% bovine serum albumin (BSA)/phosphate-buffered saline (PBS) for 1hour at 4°C, sections were incubated overnight at 4°C with 1 μg/ml of the indicated Fc fusion proteins in 0.5× block. After extensive washing, the sections were heat-treated for 30 minutes at 70°C and blocked for 1 hour in 0.5× block with 0.1% Triton X-100. Subsequently, sections were incubated with alkaline phosphatase conjugated anti-Fc antibody (1:1000; Promega) overnight at 4°C. After extensive washing with PBS/0.1% Triton X-100, binding of fusion proteins was revealed using BCIP/NBT as a substrate. Sections were counterstained with DAPI and embedded in Moviol.

Immunohistochemistry

Animals at the stages indicated were fixed for 7 days in 4% formaldehyde/PBS and then processed for immunohistochemistry using a series of IMS solutions of ascending concentration (30%, 70%, 90% to absolute). Tissue was then processed through a series of IMS/xylene (50:50), two solutions of xylene and two solutions of paraffin wax before being embedded in wax. Paraffin sections were cut (5 μm) and dewaxed overnight at 60°C. After two changes in xylene (5 minutes each), three changes in absolute IMS (2 minutes each), 70% IMS (2 minutes), sections were blocked for 10 minutes in 3% H_2O_2 followed by excess washes in tap water. Sections were pressure-cooked in 10 mM citric acid/H_2O (pH 6) for 5 minutes to retrieve antigen sites. Slides were then washed in tap water and equilibrated in 0.05 M TBS followed by blocking in 2% BSA/TBS prior to overnight incubation with a rabbit polyclonal serum against Robo, S3, diluted 1:2000 at 37°C. This antiserum was raised against a 14 amino acid peptide stretch in the Ig domain 1 of mouse Robo1, which is identical to that in mouse Robo2 with the exception of one amino acid. Specific binding of the antiserum can be blocked by pre-incubation with either the immunogen, Robo1-Fc or Robo2-Fc indicating that the serum binds both Robo1 and Robo2 (L. Bannister and V.S., unpublished). Neighbouring sections – 5 μm apart – were stained with a rabbit anti β-tubulin antibody (Cambridge Bioscience, Cambridge, UK). After washing, the primary antibody was detected using the tyramide-StreptABC/HRP method (Dako, Glostrup, Denmark) and DAB as a substrate. Sections were counterstained in Harris' Haematoxylin and dehydrated before mounting in DPX mounting medium (RA Lamb, East Sussex, UK).

Collagen assays

E14.5-E15.5 VNO explants were prepared as described by Cloutier et al. (Cloutier et al., 2002) and co-cultured with COS cell-aggregates secreting Slit1, Slit2 or Slit3 as previously described (Patel et al., 2001). Lipofection was used to transfect 6 cm^2 dishes with a total amount of 0.75 μg Slit2 DNA or 1.5 μg DNA for Slit1 and Slit3. Cultures were incubated for 2-3 days at 37°C/5% CO_2 in neurobasal medium using B27 additives (both Invitrogen, Carlsbad, CA) and recorded with phase-contrast microscopy using Lucia G software (Laboratory Imaging). Heparin was not added to the culture medium. Quantification of neurite outgrowth was carried out as described by Chen et al. (Chen et al., 2000).

Results

Robo/Slit expression in the mouse VNO

In a first step towards examining Robo/Slit function in the mouse vomeronasal projection, we performed a detailed expression analysis of Robo receptors (Robo1 and Robo2) and Slit ligands (Slit1-Slit3). We analysed their expression patterns on tissue sections using specific antisense riboprobes (Figs 1, 2 and 4), and also performed immunostaining using a Robo-

specific antibody (Fig. 5) and a Robo1-Fc fusion protein (Fig. 3). In situ hybridisation was performed at E15.5, P1, P5 and P21, which covers the period of formation of the vomeronasal projection. If not stated otherwise, the data presented are at P1 only, as we found that the principal expression patterns of Robos and Slits between E15.5 and P21 are unchanged.

The VNO is a bilaterally organised tube-like structure located beneath the nasal septum, containing sensory epithelia appearing in a crescent shape adjacent to the vomeronasal vein (Fig. 1). Robo1 and Robo2 are strongly expressed in the VNO sensory epithelium (Fig. 1A,B). Robo1 is downregulated at later stages of development (Fig. 4A). A detailed analysis shows that Robo2 and, to a lesser extent, Robo1-expressing neurones are localised in small patches, with neurones expressing varying amounts of mRNA (Fig. 1H).

The VNO also expressed Slit1 and Slit3, with Slit1 being expressed at higher levels (Fig. 1D,F). Both Slit1 and Slit3 RNAs were found in a patchy pattern, similar to that of Robos (Fig. 1G). Slit2 was not expressed in the sensory epithelium, but specifically labelled a region close to the vomeronasal vein (Fig. 1E). Expression of Slit2 in this region was undetectable by P21 (Fig. 4E).

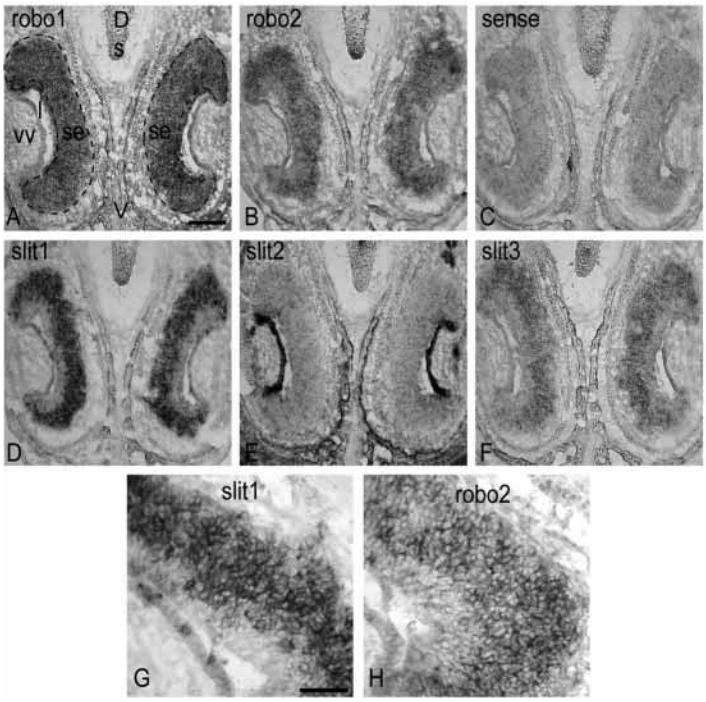

Fig. 1. Sensory neurones expressing Robo and Slit RNA are intermingled in the VNO at P1. Coronal sections through the VNO outline the sensory epithelia (se, broken line) located underneath the nasal septum (s). (A,B) Cell bodies expressing Robo1 (A) or Robo2 (B) are scattered throughout the sensory epithelia of the VNO in newborn mice. (C) Sections stained with Robo2 sense riboprobes are negative. (D,F) Slit1- (D) and Slit3 (F)-expressing cells are distributed all over the entire area of the sensory epithelia. (E) Slit2 is not expressed on the sensory epithelia, but marks the lateral margins of the VNO sensory epithelia. (G,H) Higher magnifications of B and D, indicating that individual neurones expressing Slit1 (G) and Robo2 (H) RNA are distributed in patches in the VNO sensory epithelium. D, dorsal; l, lumen; se, sensory epithelium; s, nasal septum; V, ventral; vv, vomeronasal vein. Scale-bar: 100 μm in A-F; 50 μm in G,H.

Asymmetric distribution of Slits in the mouse AOB

VNO axons entering the AOB at its medial margin (see Fig. 7) form a distinct nerve layer (n) in the dorsal part of the AOB (Fig. 2A). Mitral- and tufted (m/t) cells located in the ventral part of the AOB elaborate dendrites to establish synapses with VNO axons in glomeruli and send axons towards other regions of the brain such as the amygdala (Dulac, 2000; Keverne, 2002). The expression of RNA coding for Slit1 and Slit3 in the AOB is confined to clusters of cells at the anterior border of the AOB (arrows, Fig. 2D,F). This asymmetric distribution of Slit is preserved between E15.5 and P5, but is no longer apparent at P21 (data not shown). Slit2 is not expressed in this anterior cell group but is detected in cells scattered in the mitral/tufted (m/t) cell layer throughout the AOB, with individual cells expressing different RNA levels (Fig. 2E).

In addition, Robo2 RNA (Fig. 2B), and to a lesser extent Robo1 RNA (Fig. 2A), are uniformly expressed on m/t cells of the AOB. Robo2 is also strongly expressed on mitral and tufted cells of the main olfactory bulb (arrows, Fig. 2B). However, by using a Robo-specific antibody we observed staining of only the posterior part of the nerve layer at E15.5 (Fig. 5F), at P1, P4 (data not shown), and at P21 (Fig. 5G,H).

Given that Slits are secreted proteins, we reasoned that in particular the high punctuate expression of Slits 1 and 3 at the anterior border of the AOB might result in a differential (or graded) expression of Slit proteins within the AOB. For this purpose we have generated and used a set of Robo-Fc fusion proteins to specifically detect Slit expression. Instead of using a Robo1-Fc fusion protein containing all five Ig domains, we have used sub-domains from the extracellular part of Robo having different Slit binding capabilities (Fig. 3A,B). Based on structure-function analysis, only Ig domains 1 and 2, but not 3-5, are involved in Slit binding (V.S., unpublished). Hence, a Fc fusion protein containing Ig domains 1 and 2 (Δ3, 4, 5 Robo1-Fc) was used to localise Slit expression (Fig. 3C-E), while (Δ1, 2) Robo2-Fc lacking Ig domains 1 and 2 served as a negative control (Fig. 3F).

These analyses revealed a smooth gradient of Slit protein at the most medial part of the AOB being stronger in the anterior part and fading away towards the posterior part (Fig. 3C). More lateral to this position (Fig. 3D), Slit protein is found in the anterior but not the posterior AOB. In the central part of the AOB (Fig. 3E), there is a stronger Slit expression in the anterior part of the mitral/ tufted cell layer than in its posterior part, which is evident in approximately half of the sections taken (n>10 mice, 2-3 sections/bulbus), while in the remaining sections an even expression of Slit was found. In summary, the asymmetric expression of Slit protein is present at the time of ingrowth of vomeronasal axons into the AOB and may function to steer ingrowing basal axons away from the topographically inappropriate anterior AOB (see below).

Thus, it appears that Slits are differentially expressed in the AOB, while Robo protein – similar to the situation in the VNO (see Fig. 5B) – might be transported into the axons leaving the cell body Robo protein negative. Consistent with this, we found Robo protein on axons of the lateral olfactory tract connecting the MOB with other olfactory processing centres of the brain (see below, Fig. 5G arrows).

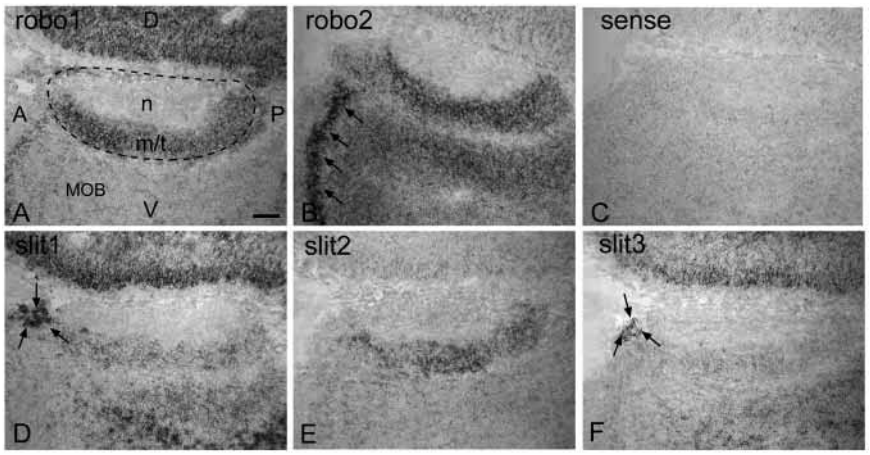

Fig. 2. RNA expression patterns of Robos and Slits in the AOB. In situ hybridisation experiments were performed on sagittal sections of the AOB at P1. The outline of the entire AOB is given by broken lines in A. VNO axons in the nerve layer (n) form synapses with mitral- and tufted cells (m/t) located ventrally in the AOB. (A,B) M/t cells along the entire anteroposterior axis of the AOB express Robo1 (A) and Robo2 (B) RNA. Robo2 is also strongly expressed in m/t cells of the MOB (arrows in B). (C) Probing AOB sections with Robo2 sense riboprobes result in no staining. (D,F) Slit1- (D) and Slit3- (F) expressing cells are concentrated at the very anterior border of the AOB (arrows). (E) By contrast, Slit2 RNA is expressed throughout the AP axis of the AOB. AOB, accessory olfactory bulb; A, anterior; D, dorsal; L, lateral; M, medial; MOB, main olfactory bulb; m/t, mitral and tufted cells; n, nerve layer; P, posterior; V, ventral. Scale bar: 100 μm.

Segregation of Robo- and Slit-expressing cells in the adult mouse VNO

At birth, presumptive apical and basal cell bodies in the VNO sensory epithelium are intermingled as revealed by a number of markers including specific Gα subunits (Berghard and Buck, 1996; Berghard et al., 1996; Jia and Halpern, 1996). This intermingling is resolved during the first postnatal weeks, when apical and basal cell bodies become confined to their respective zones in the VNO. To investigate a possible change in Robo and Slit RNA expression that might coincide with this process, in situ hybridisation experiments were performed at P21 (Fig. 4). Compared with earlier stages (Fig. 1), Robo2 expression is now confined to the basal zone of the VNO (Fig. 4B), but its expression level varies between individual cells (Fig. 4C). By contrast, Robo1 expression is downregulated as early as P5 (data not shown) and hardly detectable at P21 (Fig. 4A). The expression of Slits is more restricted compared to earlier stages, with Slit3 mostly confined to the apical VNO and Slit1 having a higher expression in the apical than the basal VNO (Fig. 4D,F).

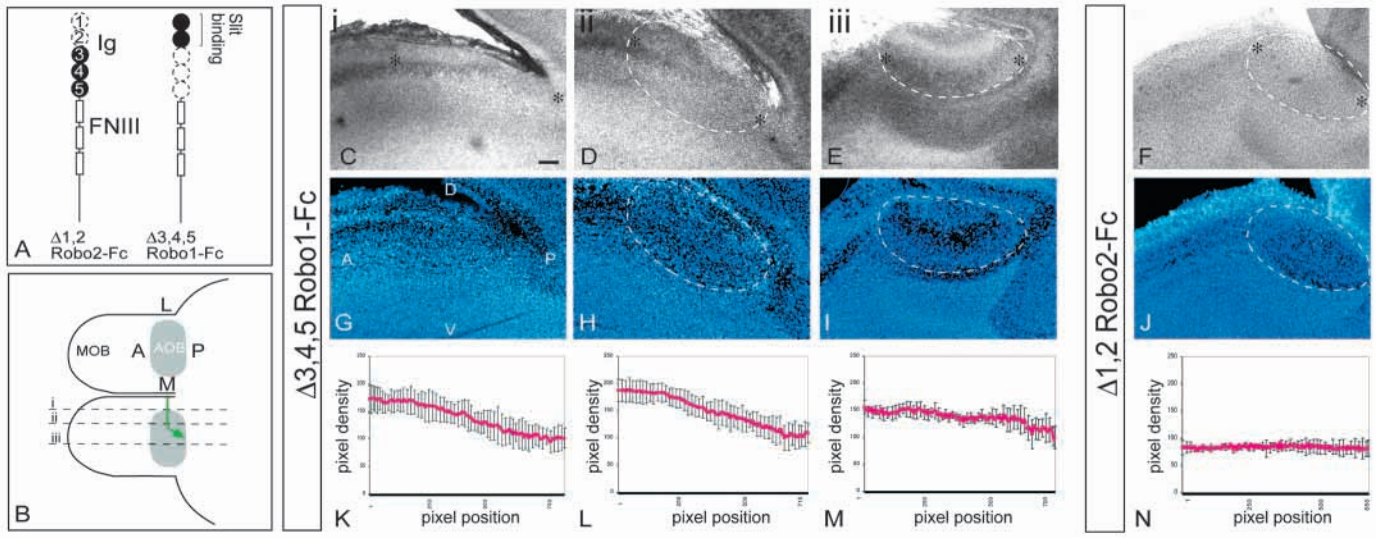

Fig. 3. Differential expression of Slit proteins in the AOB. The experiments were carried out on sagittal sections of the AOB at P1. (A) Schematic drawing of the probes used. As Ig domains 1 and 2 confer Slit binding, a deletion construct omitting these two domains named (Δ1,2)-Robo1-Fc was used as a control, while (Δ3,4,5)-Robo2-Fc containing Ig domains 1 and 2 was used to detect Slit protein expression. (B) Dorsal view of the AOB. Basal vomeronasal axons (green) invade the AOB from its medial margin and project onto the posterior AOB. Approximate location of sagittal sections shown in C,D,E are indicated by broken lines i, ii and iii, respectively. (C,D,E) Detection of Slit proteins using (Δ3,4,5) Robo1-Fc on 150 μm sagittal vibratome sections. Their approximate positions along the mediolateral axis (i,ii,iii) are shown in B. Bound (Δ3,4,5) Robo1-Fc was visualised using an alkaline phosphatase conjugated anti-Fc specific antibody. (G-I) Corresponding DAPI stainings to C,D,E. (F,J) Staining with (Δ1,2) Robo2-Fc (F) serving as a negative control and the corresponding DAPI staining (J). (K-N) Quantification of staining patterns shown in C-F using the Phoretix ID Quantifier V4.0 program. Here, the staining intensity of the area between the two asterisks shown in C-F, which covers the AOB along its entire anteroposterior dimension, was measured. Graphs show average values and standard deviations. K shows the results from the measurement of six comparable sections (n=6) at the level of i, of which C is a typical example (n=10 for L, n=6 for M and n=3 for N). These data indicate a stronger expression of Slits in the anterior than the posterior AOB. AOB, accessory olfactory bulb; A, anterior; D, dorsal; L, lateral; M, medial; MOB, main olfactory bulb; P, posterior; V, ventral. Scale-bar: 100 μm in C-J.

Expression of Robo protein on basal VNO axons

Given its function as an axon guidance receptor, we wished to determine the localisation of Robo protein within the vomeronasal projection by immunohistochemistry using an antibody, which detects both Robo1 and Robo2 (Hivert et al., 2002) (see Materials and methods for details) on tissue sections.

At E15.5, VNO axons emanating from the VNO sensory epithelium and navigating dorsally along the nasal septum towards the AOB are strongly Robo positive (arrows, Fig. 5A,B). In the AOB, we observed stronger staining for Robo in the posterior than in the anterior part of the nerve layer (arrows, Fig. 5F). This is particularly interesting as this zone-specific localisation occurs prior to the segregation of the corresponding cell bodies in the VNO. In addition, we observed a differential expression of Robo across the mediolateral (ML) axis of the AOB at E15.5 (Fig. 5D) and P1 (data not shown). Here, the lateral aspect of the nerve layer shows higher Robo staining than its medial side, from which VNO axons enter the AOB (arrows, Fig. 5D; Fig. 7). However, this pattern is transient and by P21 there is no longer a differential distribution of Robo along the ML axis (data not shown).

Inspection of sagittal sections of the AOB at P21 shows that only the posterior half of the AOB nerve layer – which is formed by basal axons – is Robo positive (Fig. 5G,H; Fig. 7).

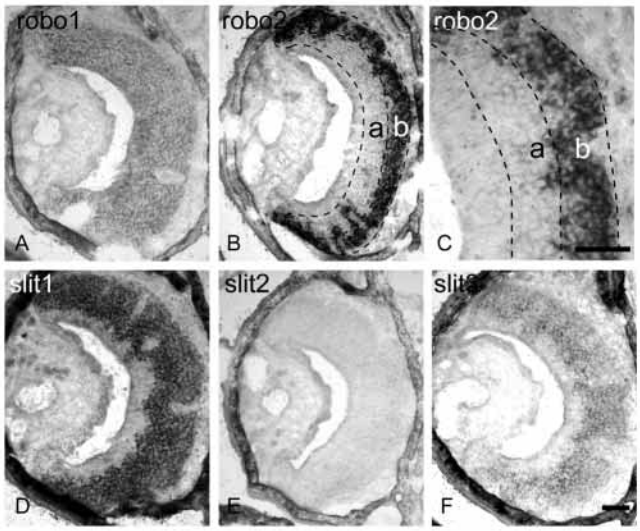

Fig. 4. Segregation of Robo- and Slit-expressing neurones in the VNO at P21. After ~2 weeks of postnatal development, sensory neurones are restricted to either the apical (a) or basal zone (b) of the VNO sensory epithelium (B) (see also Fig.7). All pictures depict coronal sections of one half of the VNO. (A) Only residual levels of Robo1 RNA are detectable on both apical and basal cell bodies. (B) By contrast, Robo2 expression is prominent and confined to the basal zone of the VNO sensory epithelium. (C) Higher magnification of B, demonstrating the restriction of Robo2-RNA to basal sensory neurones. Note also the patches of Robo2-expressing neurones in the basal zone. (D,F) Slit1 (D) is more strongly expressed in the apical than basal VNO, while Slit3 RNA (F) is mainly restricted to cell bodies of the apical zone. (E) Slit2 RNA, which was labelling the lateral VNO at P1 (see Fig. 1E), has disappeared at P21. a, apical; b, basal, D, dorsal; V, ventral. Scale bars: in F, 100 μm for A,B,D-F; in C, 50 μm for C.

These data are consistent with the expression of Robo2 RNA in the basal zone of the VNO and the downregulation of Robo1 RNA at P21 (Fig. 4).

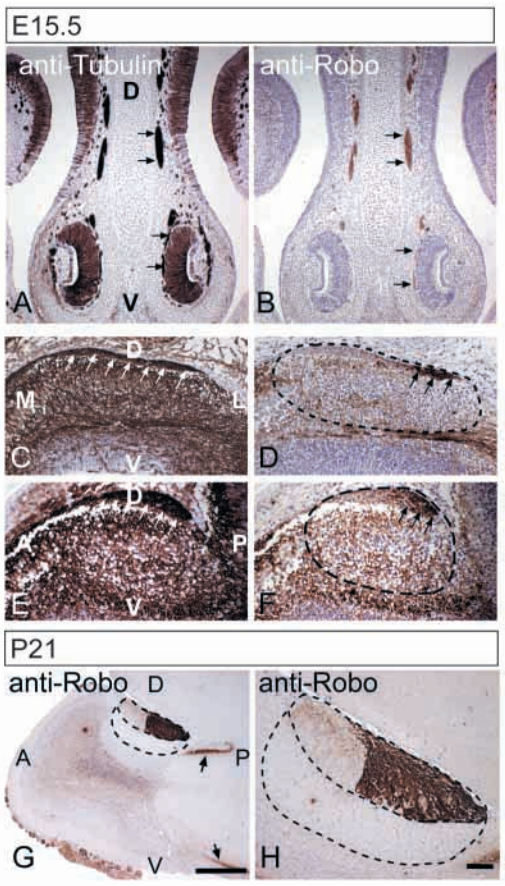

Fig. 5. Localisation of Robo protein in the VNO and AOB. The expression of Robo protein was examined at E15.5 (A-F) and P21 (G,H) using a Robo specific antiserum (B,D,F-H) on paraffin wax sections. Neighbouring sections (5 μm apart) were stained for β-tubulin (A,C,E). The outline of the AOB is highlighted by a broken line in G,H. (A,B) VNO axons (stained for tubulin in A) leave the sensory epithelia of the VNO on both sides and navigate dorsally along the nasal septum. These axons clearly express Robo protein (arrows A,B). Note the absence of Robo protein from the cell bodies of the sensory epithelium. (C,D) Analysis of Robo expression (D) along the mediolateral axis of the AOB. Coronal sections through the AOB reveal a stronger Robo expression on the lateral than on the medial region of the VNO nerve layer (arrows in D). (C) The entire length of the VNO nerve layer is indicated by white arrows. (E,F) Robo expression (F) along the anteroposterior axis of the AOB. On a sagittal section Robo staining is mostly confined to the posterior extent of the nerve layer in the AOB (arrows). Importantly, we find this expression already at E15.5, despite the fact that basal neurones are still intermingled with apical neurones within the VNO sensory epithelium. The entire extent of the nerve layer is shown on a neighbouring section stained for tubulin (see arrows in E). (G,H) At P21, Robo protein is clearly restricted to the nerve layer of the posterior AOB, conclusively demonstrating that only the basal subpopulation of VNO axons innervating the posterior half of the AOB expresses Robo. Axons of the main sensory epithelium terminating in glomeruli of the main olfactory bulb also express Robo (G). Arrows in G indicate the expression of Robo in the lateral olfactory tract. A, anterior; D, dorsal; P, posterior; V, ventral Scale-bar: in G, 1 mm for A,C,E,G; in H, 100 μm for B,D,F,H.

Finally, axons of the main olfactory bulb, which terminate in glomeruli of the ventral part of the main olfactory bulb, are also Robo positive (Fig. 5G), suggesting that Robos and Slits may also be involved in the topographic mapping in the main olfactory system.

Robo-Slit interactions repel vomeronasal axons

The expression profile presented in this study suggests that basal VNO axons are guided to the posterior AOB based on a chemorepulsive effect exerted by a differential Slit expression in the AOB. To investigate this idea more directly, we analysed the sensitivity of VNO axons to all three Slits in a collagen gel co-culture system. Here, E14.5 VNO explants were arranged in proximity to COS cell aggregates secreting Slit1, Slit2 or Slit 3 or mock-transfected control cells (Fig. 6, see Materials and methods). Two to 3 days later, the response of VNO axons to the cell clusters was monitored. In control experiments using mock-transfected COS cell aggregates (Fig. 6A, n=33), we observed an almost radially symmetrical outgrowth of VNO axons indicating an insignificant level of secretion of repulsive molecules by COS cells per se (Fig. 6A). By contrast, VNO axons were robustly repelled from Slit-secreting COS cell aggregates, with virtually no axons growing towards the Slit-producing cells (Fig. 6B-D). This chemorepulsion was observed even without the addition to the growth medium of heparin, which is known to enhance Slit release into the medium (Brose et al., 1999; Nguyen Ba-Charvet et al., 1999; Hu, 2001).

Subsequently, the repulsive effects of Slit1-Slit3 on vomeronasal axons were quantified in more detail. We compared the extent of axon-outgrowth in the proximal and distal quadrants (P/D ratio) of VNO explants, summarised in Fig. 6E (Chen et al., 2000). A P/D ratio of 1 means that there is no repulsion, whereas lower P/D values indicate chemorepulsion. For controls (mock transfection), we determined a P/D ratio of 0.82 [±0.18 (s.e.m.)] indicating very little repulsive activity of COS cells on vomeronasal axons per se. However, the P/D ratio for experiments using Slit-transfected cells was drastically reduced with ratios of 0.25 (±0.13), 0.1 (±0.11) and 0.25 (±0.18) for Slit1, Slit2 and Slit3, respectively. This indicates a statistically significant repulsive activity of all three Slits on VNO axons, when compared with controls (P<0.01, t-test, Fig. 6E). This finding is consistent with data showing that Robo1 is uniformly expressed in the VNO during embryonic stages (Fig. 1A, data not shown), presumably conferring sensitivity to Slits on all VNO axons in the collagen assays despite the basal expression of Robo2.

Discussion

The vomeronasal projection is topographically organised such that axons from the apical VNO project onto the anterior AOB and axons from the basal VNO connect to the posterior AOB. Although targeting of apical axons is governed by axonally expressed ephrin A proteins using an attractive guidance mechanism, and also by neuropilins, it was unclear how basal axons are directed to their targets. Differential expression patterns of Slits and their Robo receptors as well as a chemorepulsive effect of Slits on vomeronasal axons renders this family of axon guidance molecules into a promising candidate for performing this task.

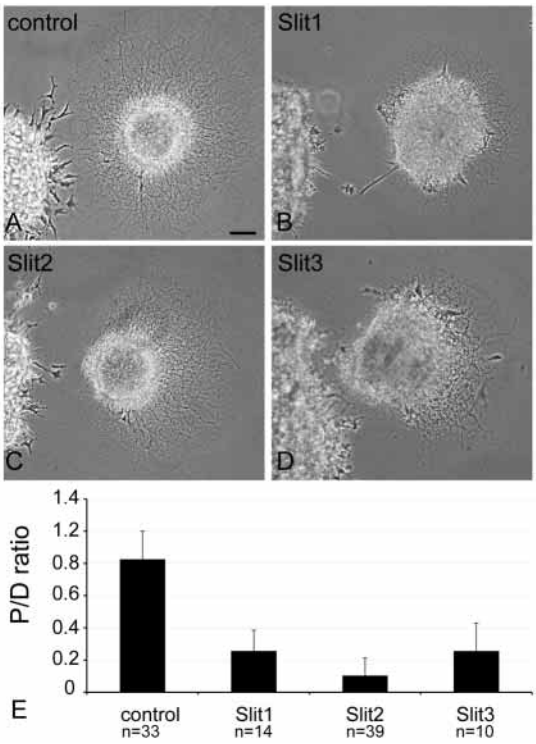

Fig. 6. Slits guide VNO axons by chemorepulsion. E14.5 VNO explants were placed in a collagen-matrix next to COS cell aggregates transfected with Slit1 (B), Slit2 (C), Slit3 (D) or mock transfected (control, A). Lipofection was used to transfect 6 cm^2 dishes with a total amount of 0.75 μg Slit2 DNA and 1.5 μg DNA for Slit1 and Slit3. After 3 days in culture, outgrowth of VNO axons was recorded and quantified (E). (A) Axon-outgrowth from VNO explants was radial and not influenced by mock-transfected COS cells (n=33 explants). (B-D) Slit1-Slit3 caused chemorepulsion of VNO axons. (E) The repulsive effect of Slit1-Slit3 on VNO axons was quantified by measuring the length of the neurite front in the proximal (P) and distal quadrants (D) of the VNO explant relative to the cell aggregate. In controls, a P/D ratio of ~1 (0.82±0.18) indicates almost no repulsive activity of mock-transfected cell aggregates. By contrast, Slit1-Slit3 shift the P/D ratio to 0.25±0.13, 0.1±0.11 and 0.25±0.18, respectively, indicating a strong Slit-mediated chemorepulsion of VNO axons. Scale bar: 100 μm.

Robo and Slit expression patterns

We have shown that Robo receptors are expressed on vomeronasal axons throughout the time at which this topographic projection is formed. During early stages of development of this projection (P1) differential expression patterns of Robos on apical versus basal axons are difficult to analyse, because cell bodies from presumptive basal and apical axons are intermingled within the VNO. Nevertheless, the patchy expression of Robo2 mRNA in particular is in agreement with such a differential expression on apical versus basal cell bodies. Robo1, however, appears to be rather uniformly expressed in the VNO. At later stages of development, when apical and basal cell bodies in the VNO have separated, Robo2 is obviously expressed only on basal axons, while Robo1 expression is no longer detectable.

These data were confirmed by staining vomeronasal axons

during their growth into the AOB, which uncovered a stronger Robo protein staining in the posterior AOB, the target area of basal axons, than in its anterior part. This indicates that – given that targeting of vomeronasal axons is topographically specific from the beginning – basal axons express Robo receptors more strongly than apical axons from early stages of development. Our data therefore suggest that basal axons are more sensitive to Slits than are apical ones and might react differently in a target area of differential Slit expression.

The VNO also expressed Slit1 and Slit3 mRNA, with the former being expressed at higher levels than the latter. It is unknown whether the apparent co-expression of Slits with Robos on sensory VNO neurones exerts any effects on the sensitivity of these axons. Co-expression of Eph receptors and ephrins on nasal retinal ganglion cell axons renders these axons less sensitive to exogenously applied ephrin As (Hornberger et al., 1999).

To uncover any differential Slit protein expression pattern in the AOB, we have used a (Δ3,4,5) Robo1-Fc fusion protein binding to all three Slits, to probe sections from the AOB and demonstrated a differential protein localisation of Slits in the AOB such that their concentration was higher in the anterior than posterior part. This fits with the (stronger) Slit1 and (weaker) Slit3 RNA expression at its anterior border, possibly in so-called necklace glomeruli (Lipscomb et al., 2002; Shinoda et al., 1989). The actual contribution of Slit1 and Slit3 to this differential expression can not be revealed by this staining method and might require suitable antibodies (Rajagopalan et al., 2000; Simpson et al., 2000).

Vomeronasal axons are chemorepulsed by Slits

Functional investigation of the interaction of Slits with Robo-expressing vomeronasal axons in collagen co-cultures showed a chemorepulsive activity of all three Slits on vomeronasal axons from E14.5 explants. Given that at E15.5 Robo2 is restricted to basal axons only, while Robo1 is uniformly expressed on both apical and basal axons, one might have expected a certain differential sensitivity of basal versus apical axons, which we did not observe. This might reflect technical limitations of the collagen gel assay and its quantification, which result in a failure to detect subtle differences in sensitivity.

Importantly, the collagen co-culture assays could be performed only at early embryonic stages (i.e. E14-E15.5), as at later (postnatal) stages there is little axon outgrowth from VNO explants. However, at early stages, the difference in Robo expression between apical and basal vomeronasal axons appears to be much smaller than at later stages. In particular, the expression level of the uniformly expressed Robo1 appears to be somewhat higher than that of the differentially expressed Robo2 (Fig. 1; and data not shown for E15.5). At later stages of development, i.e. at crucial times of topographic map formation, Robo1 expression is significantly downregulated, while the differential Robo2 expression is unchanged. Thus, we would expect a differential sensitivity of apical versus basal VNO axons in collagen co-culture assays for explants from older mice. However, as mentioned, the lack of axon outgrowth from postnatal VNO explants prevents us from demonstrating the anticipated difference in apical versus basal VNO axon sensitivity in vitro.

Segregation of basal and apical VNO axons in the AOB

The expression patterns of ephrin A/Ephs and Robos/Slits suggest a mechanism by which basal and apical axons are guided to the posterior and anterior AOB respectively. According to this model, guidance would result from the sum of attractive forces exerted by the ephrin A/Eph system and the repulsive forces acting via the Slit/Robo system, which appear to be different for apical versus basal axons.

We propose that vomeronasal axons arrive at the AOB and diverge at the medial margin between the anterior and posterior zones (see Fig. 7). Here, apical axons, which express higher concentrations of ephrin As than basal ones, turn into the anterior AOB, because of an attraction towards higher concentrations of EphA receptors in the anterior AOB (Knöll et al., 2001). Given that basal axons also express ephrin A proteins, they in principle would also turn into the anterior AOB. However, because these basal axons express higher concentrations of Robo receptors than apical axons, they would be repelled from invading the anterior AOB, which contains higher concentrations of Slit, and turn into the posterior AOB (for details see Fig. 7).

The neuropilin 2/semaphorin class 3 axon guidance family contributes also to the guidance of apical axons, possibly via a chemorepulsive mechanism involving a semaphorin gradient through differential neuropilin/semaphorin sequestering (Cloutier et al., 2000; Walz et al., 2002).

Interplay between axon guidance molecules and vomeronasal receptors

A subsequent step in the formation of the vomeronasal projection is the establishment of vomeronasal receptor-specific, complex patterns of glomeruli within the anterior and posterior zones, which requires the expression of the vomeronasal receptors themselves (Belluscio et al., 1999; Rodriguez et al., 1999). A role of ‘classical’ axon guidance molecules in this fine-tuning process appears possible and is consistent with the patchy expression of Robo2 (shown here) and of ephrin A5 (Knöll et al., 2001) in the basal and apical VNO, respectively. This could lead to differential sensitivities within the subpopulations of apical and basal axons, and might lead to a differential targeting within the two zones of the AOB.

The development of the zonal topography

One of the special features of the vomeronasal system is the intermingling of future apical and basal cell bodies in the VNO during early development, and their subsequent separation during postnatal development. We show that at the time when VNO cell bodies are still intermingled, the ingrowth of axons into the AOB is already topographic or zone-specific. This is evident from immunohistochemical analyses showing that Robo staining is largely restricted to the posterior AOB already at E15.5 (Fig. 5) and P1 (data not shown). Thus, the segregation of apical and basal cell bodies in the VNO is not a precondition for the zone-specific targeting of their respective axons within the AOB. Robo is one of the earliest markers that defines the zonal projection of vomeronasal axons, and might therefore be particularly suited to investigate further details on the formation of the zonal projection of vomeronasal axons.

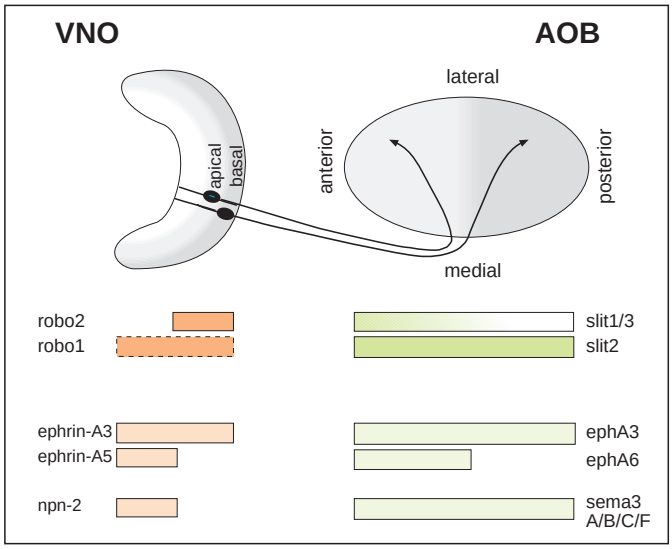

Fig. 7. Summary of the expression patterns of guidance molecules involved in the zone-to-zone targeting of vomeronasal axons. The upper part depicts schematically the zone-to-zone projection in the vomeronasal system. Axons from the apical zone of the VNO terminate in the anterior AOB, whereas basal axons terminate in the posterior AOB. Note that apical and basal axons enter the AOB at its medial margin. The lower part summarises the expression patterns of three families of axon guidance molecules described so far in the vomeronasal projection. The expression patterns provided in this study suggest that Robos and Slits act predominantly on basal axons. Robo2 appears to be the principal guidance receptor for basal axons, whereas Robo1 is uniformly expressed and later downregulated, leaving only faint expression on both apical and basal axons (broken line). This suggests a model in which basal axons expressing Robos more strongly than apical axons navigate to the posterior AOB due to repulsive interactions, with Slit proteins secreted from the anterior AOB. Ephrin A proteins and neuropilin 2 instead operate mainly on the apical subpopulation of VNO axons. Apical axons with higher ephrin A expression levels than basal axons project to the anterior AOB, with express higher concentrations of Epha proteins than the posterior AOB. In this scheme, Epha/ephrin A interactions would guide VNO axons on the basis of an attractive guidance mechanism, consistent with data from the stripe assay (Knöll et al., 2001). In turn, apical axons expressing neuropilin 2 are repelled by class 3 semaphorins, which are uniformly localised in the AOB. Neuropilin 2 in the anterior AOB might sequester semaphorins, thus rendering apical axons sensitive to only the semaphorins in the posterior AOB (Cloutier et al., 2000; Walz et al., 2002).

Potential functions of Robos in the adult vomeronasal projection

It is known that the vomeronasal projection is continuously renewed throughout life (Barber and Raisman, 1978; Gogos et al., 2000; Graziadei and Graziadei, 1979; Graziadei et al., 1978; Martinez-Marcos et al., 2000; Moulton, 1974). The expression of Robo2 and ephrin A5 on VNO axons of adult mice might reflect an involvement of these molecules in the guidance of later-forming axons. We observed a downregulation of Slit1, Slit3 and Epha6 in the postnatal AOB. Thus, the zone-specific guidance might be maintained through a mechanism different from the one used initially and could involve a Robo2-mediated fasciculation of VNO axons along the axonal tracts established earlier in development (Hivert et al., 2002).

Interactions between guidance families

Several different guidance molecules such as Robo, ephrin A and neuropilin proteins are expressed in overlapping and complementary expression patterns on VNO axons and were shown to be functionally involved in the zonal targeting of VNO axons in the AOB. Thus the vomeronasal system provides – owing to its clear-cut zonal bipartition – an excellent and simple model system with which to study the integration of attractive and repulsive signalling pathways controlled by these molecules.

This work was supported by the Wellcome Trust. B.K. was supported by a Fellowship of the Deutsche Forschungsgemeinschaft (DFG), and H.S. by a Marie Curie Fellowship of the European Commission. We are grateful to Adelaide Annan for her generous help and technical expertise. We thank Marc Tessier-Lavigne for reagents, and Franco Weth for valuable comments on the manuscript.

References

Bagri, A., Marin, O., Plump, A. S., Mak, J., Pleasure, S. J., Rubenstein, J. L. and Tessier-Lavigne, M. (2002). Slit proteins prevent midline crossing and determine the dorsoventral position of major axonal pathways in the mammalian forebrain. *Neuron* **33**, 233-248.

Barber, P. C. and Raisman, G. (1978). Cell division in the vomeronasal organ of the adult mouse. *Brain Res.* **141**, 57-66.

Belluscio, L., Koentges, G., Axel, R. and Dulac, C. (1999). A map of pheromone receptor activation in the mammalian brain. *Cell* **97**, 209-220.

Berghard, A. and Buck, L. B. (1996). Sensory transduction in vomeronasal neurons: evidence for G alpha o, G alpha i2, and adenylyl cyclase II as major components of a pheromone signaling cascade. *J. Neurosci.* **16**, 909-918.

Berghard, A., Buck, L. B. and Liman, E. R. (1996). Evidence for distinct signaling mechanisms in two mammalian olfactory sense organs. *Proc. Natl. Acad. Sci. USA* **93**, 2365-2369.

Brose, K., Bland, K. S., Wang, K. H., Arnott, D., Henzel, W., Goodman, C. S., Tessier-Lavigne, M. and Kidd, T. (1999). Slit proteins bind Robo receptors and have an evolutionarily conserved role in repulsive axon guidance. *Cell* **96**, 795-806.

Brose, K. and Tessier-Lavigne, M. (2000). Slit proteins: key regulators of axon guidance, axonal branching, and cell migration. *Curr. Opin. Neurobiol.* **10**, 95-102.

Chen, H., Bagri, A., Zupicich, J. A., Zou, Y., Stoeckli, E., Pleasure, S. J., Lowenstein, D. H., Skarnes, W. C., Chedotal, A. and Tessier-Lavigne, M. (2000). Neuropilin-2 regulates the development of selective cranial and sensory nerves and hippocampal mossy fiber projections. *Neuron* **25**, 43-56.

Cloutier, J.-F., Giger, R. J., Koentges, G., Dulac, C., Kolodkin, A. L. and Ginty, D. D. (2000). Neuropilin-2 mediates axonal fasciculation, zonal segregation, but not axonal convergence, of primary accessory olfactory neurons. *Neuron* **33**, 877-892.

Conover, J. C., Doetsch, F., Garcia-Verdugo, J. M., Gale, N. W., Yancopoulos, G. D. and Alvarez-Buylla, A. (2000). Disruption of Eph/ephrin signaling affects migration and proliferation in the adult subventricular zone. *Nat. Neurosci.* **3**, 1091-1097.

Del Punta, K., Leinders-Zufall, T., Rodriguez, I., Jukam, D., Wysocki, C. J., Ogawa, S., Zufall, F. and Mombaerts, P. (2002a). Deficient pheromone responses in mice lacking a cluster of vomeronasal receptor genes. *Nature* **419**, 70-74.

Del Punta, K., Puche, A., Adams, N. C., Rodriguez, I. and Mombaerts, P. (2002b). A divergent pattern of sensory axonal projections is rendered convergent by second-order neurons in the accessory olfactory bulb. *Neuron* **35**, 1057-1066.

Dulac, C. (2000). Sensory coding of pheromone signals in mammals. *Curr. Opin. Neurobiol.* **10**, 511-518.

Dulac, C. and Axel, R. (1995). A novel family of genes encoding putative pheromone receptors in mammals. *Cell* **83**, 195-206.

Erskine, L., Williams, S. E., Brose, K., Kidd, T., Rachel, R. A., Goodman, C. S., Tessier-Lavigne, M. and Mason, C. A. (2000). Retinal ganglion cell

axon guidance in the mouse optic chiasm: expression and function of robos and slits. *J. Neurosci.* **20**, 4975-4982.

Fricke, C., Lee, J. S., Geiger-Rudolph, S., Bonhoeffer, F. and Chien, C. B. (2001). astray, a zebrafish roundabout homolog required for retinal axon guidance. *Science* **292**, 507-510.

Georgiou, M. and Tear, G. (2002). Commissureless is required both in commissural neurones and midline cells for axon guidance across the midline. *Development* **129**, 2947-2956.

Gogos, J. A., Osborne, J., Nemes, A., Mendelsohn, M. and Axel, R. (2000). Genetic ablation and restoration of the olfactory topographic map. *Cell* **103**, 609-620.

Graziadei, P. P., Levine, R. R. and Graziadei, G. A. (1978). Regeneration of olfactory axons and synapse formation in the forebrain after bulbectomy in neonatal mice. *Proc. Natl. Acad. Sci. USA* **75**, 5230-5234.

Graziadei, G. A. and Graziadei, P. P. (1979). Neurogenesis and neuron regeneration in the olfactory system of mammals. II. Degeneration and reconstitution of the olfactory sensory neurons after axotomy. *J. Neurocytol.* **8**, 197-213.

Guthrie, S. (2001). Axon guidance: Robos make the rules. *Curr. Biol.* **11**, R300-R303.

Herrada, G. and Dulac, C. (1997). A novel family of putative pheromone receptors in mammals with a topographically organized and sexually dimorphic distribution. *Cell* **90**, 763-773.

Hivert, B., Liu, Z., Chuang, C. Y., Doherty, P. and Sundaresan, V. (2002). Robo1 and robo2 are homophilic binding molecules that promote axonal growth. *Mol. Cell Neurosci.* **21**, 534-545.

Holmes, G. P., Negus, K., Burridge, L., Raman, S., Algar, E., Yamada, T. and Little, M. H. (1998). Distinct but overlapping expression patterns of two vertebrate slit homologs implies functional roles in CNS development and organogenesis. *Mech. Dev.* **79**, 57-72.

Hornberger, M. R., Dutting, D., Ciossek, T., Yamada, T., Handwerker, C., Lang, S., Weth, F., Huf, J., Wessel, R., Logan, C. et al. (1999). Modulation of EphA receptor function by coexpressed ephrinA ligands on retinal ganglion cell axons. *Neuron* **22**, 731-742.

Hu, H. (2001). Cell-surface heparan sulfate is involved in the repulsive guidance activities of Slit2 protein. *Nat. Neurosci.* **4**, 695-701.

Hutson, L. D. and Chien, C. B. (2002). Pathfinding and error correction by retinal axons: the role of astray/robo2. *Neuron* **33**, 205-217.

Itoh, A., Miyabayashi, T., Ohno, M. and Sakano, S. (1998). Cloning and expressions of three mammalian homologues of Drosophila slit suggest possible roles for Slit in the formation and maintenance of the nervous system. *Mol. Brain Res.* **62**, 175-186.

Jia, C. and Halpern, M. (1996). Subclasses of vomeronasal receptor neurons: differential expression of G proteins [Gi alpha 2 and G(o alpha)] and segregated projections to the accessory olfactory bulb. *Brain Res.* **719**, 117-128.

Keleman, K., Rajagopalan, S., Cleppien, D., Teis, D., Paiha, K., Huber, L. A., Technau, G. M. and Dickson, B. J. (2002). Comm sorts robo to control axon guidance at the Drosophila midline. *Cell* **110**, 415-427.

Keverne, E. B. (1999). The vomeronasal organ. *Science* **286**, 716-720.

Keverne, E. B. (2002). Mammalian pheromones: from genes to behaviour. *Curr. Biol.* **12**, R807-R809.

Kidd, T., Brose, K., Mitchell, K. J., Fetter, R. D., Tessier-Lavigne, M., Goodman, C. S. and Tear, G. (1998a). Roundabout controls axon crossing of the CNS midline and defines a novel subfamily of evolutionarily conserved guidance receptors. *Cell* **92**, 205-215.

Kidd, T., Russell, C., Goodman, C. S. and Tear, G. (1998b). Dosage-sensitive and complementary functions of roundabout and commissureless control axon crossing of the CNS midline. *Neuron* **20**, 25-33.

Knöll, B. and Drescher, U. (2002). Ephrin-As as receptors in topographic projections. *Trends Neurosci.* **25**, 145-149.

Knöll, B., Zarbalis, Z., Wurst, W. and Drescher, U. (2001). A role for the EphA family in the topographic targeting of vomeronasal axons. *Development* **128**, 895-906.

Leypold, B. G., Yu, C. R., Leinders-Zufall, T., Kim, M. M., Zufall, F. and Axel, R. (2002). Altered sexual and social behaviors in trp2 mutant mice. *Proc. Natl. Acad. Sci. USA* **99**, 6376-6381.

Li, H. S., Chen, J. H., Wu, W., Fagaly, T., Zhou, L., Yuan, W., Dupuis, S., Jiang, Z. H., Nash, W., Gick, C. et al. (1999). Vertebrate slit, a secreted ligand for the transmembrane protein roundabout, is a repellent for olfactory bulb axons. *Cell* **96**, 807-818.

Lipscomb, B. W., Treloar, H. B. and Greer, C. A. (2002). Novel microglomerular structures in the olfactory bulb of mice. *J. Neurosci.* **22**, 766-774.

Marillat, V., Cases, O., Nguyen-Ba-Charvet, K. T., Tessier-Lavigne, M., Sotelo, C. and Chedotal, A. (2002). Spatiotemporal expression patterns of slit and robo genes in the rat brain. *J. Comp. Neurol.* **442**, 130-155.

Martinez-Marcos, A., Ubeda-Banon, I., Deng, L. and Halpern, M. (2000). Neurogenesis in the vomeronasal epithelium of adult rats: evidence for different mechanisms for growth and neuronal turnover. *J. Neurobiol.* **44**, 423-435.

Matsunami, H. and Buck, L. B. (1997). A multigene family encoding a diverse array of putative pheromone receptors in mammals. *Cell* **90**, 775-784.

Mombaerts, P. (1999). Seven-transmembrane proteins as odorant and chemosensory receptors. *Science* **286**, 707-711.

Moulton, D. G. (1974). Dynamics of cell populations in the olfactory epithelium. *Ann. New York Acad. Sci.* **237**, 52-61.

Myat, A., Henry, P., McCabe, V., Flintoft, L., Rotin, D. and Tear, G. (2002). Drosophila Nedd4, a ubiquitin ligase, is recruited by Commissureless to control cell surface levels of the roundabout receptor. *Neuron* **35**, 447-459.

Nguyen Ba-Charvet, K. T., Brose, K., Marillat, V., Kidd, T., Goodman, C. S., Tessier-Lavigne, M., Sotelo, C. and Chedotal, A. (1999). Slit2-mediated chemorepulsion and collapse of developing forebrain axons. *Neuron* **22**, 463-473.

Nguyen-Ba-Charvet, K. T. and Chedotal, A. (2002). Role of Slit proteins in the vertebrate brain. *J. Physiol. Paris* **96**, 91-98.

Niclou, S. P., Jia, L. and Raper, J. A. (2000). Slit2 is a repellent for retinal ganglion cell axons. *J. Neurosci.* **20**, 4962-4974.

Patel, K., Nash, J. A., Itoh, A., Liu, Z., Sundaresan, V. and Pini, A. (2001). Slit proteins are not dominant chemorepellents for olfactory tract and spinal motor axons. *Development* **128**, 5031-5037.

Plump, A. S., Erskine, L., Sabatier, C., Brose, K., Epstein, C. J., Goodman, C. S., Mason, C. A. and Tessier-Lavigne, M. (2002). Slit1 and Slit2 cooperate to prevent premature midline crossing of retinal axons in the mouse visual system. *Neuron* **33**, 219-232.

Rajagopalan, S., Vivancos, V., Nicolas, E. and Dickson, B. J. (2000). Selecting a longitudinal pathway: Robo receptors specify the lateral position of axons in the Drosophila CNS. *Cell* **103**, 1033-1045.

Ringstedt, T., Braisted, J. E., Brose, K., Kidd, T., Goodman, C., Tessier-Lavigne, M. and O'Leary, D. D. M. (2000). Slit inhibition of retinal axon growth and its role in retinal axon pathfinding and innervation patterns in the diencephalon. *J. Neurosci.* **20**, 4983-4991.

Rodriguez, I., Feinstein, P. and Mombaerts, P. (1999). Variable patterns of axonal projections of sensory neurons in the mouse vomeronasal system. *Cell* **97**, 199-208.

Rodriguez, I., Greer, C. A., Mok, M. Y. and Mombaerts, P. (2000). A putative pheromone receptor gene expressed in human olfactory mucosa. *Nat. Genet.* **26**, 18-19.

Ryba, N. J. and Tirindelli, R. (1997). A new multigene family of putative pheromone receptors. *Neuron* **19**, 371-379.

Schimmelpfeng, K., Gogel, S. and Klambt, C. (2001). The function of leak and kuzbanian during growth cone and cell migration. *Mech. Dev.* **106**, 25-36.

Shinoda, K., Shiotani, Y. and Osawa, Y. (1989). "Necklace olfactory glomeruli" form unique components of the rat primary olfactory system. *J. Comp. Neurol.* **284**, 362-373.

Simpson, J. H., Bland, K. S., Fetter, R. D. and Goodman, C. S. (2000). Short-range and long-range guidance by Slit and its Robo receptors: a combinatorial code of Robo receptors controls lateral position. *Cell* **103**, 1019-1032.

Stowers, L., Holy, T. E., Meister, M., Dulac, C. and Koentges, G. (2002). Loss of sex discrimination and male-male aggression in mice deficient for TRP2. *Science* **295**, 1493-1500.

Sundaresan, V., Roberts, I., Bateman, A., Bankier, A., Sheppard, M., Hobbs, C., Xiong, J., Minna, J., Latif, F., Lerman, M. et al. (1998). The DUTT1 gene, a novel NCAM family member is expressed in developing murine neural tissues and has an unusually broad pattern of expression. *Mol. Cell Neurosci.* **11**, 29-35.

Tear, G. (1999). Axon guidance at the central nervous system midline. *Cell Mol. Life Sci.* **55**, 1365-1376.

Tear, G., Harris, R., Sutaria, S., Kilomanski, K., Goodman, C. S. and Seeger, M. A. (1996). *commissureless* controls growth cone guidance across the CNS midline in Drosophila and encodes a novel membrane protein. *Neuron* **16**, 501-514.

Walz, A., Rodriguez, I. and Mombaerts, P. (2002). Aberrant sensory innervation of the olfactory bulb in neuropilin-2 mutant mice. *J. Neurosci.* **22**, 4025-4035.

Yuan, S. S., Cox, L. A., Dasika, G. K. and Lee, E. Y. (1999a). Cloning and

functional studies of a novel gene aberrantly expressed in RB-deficient embryos. *Dev. Biol*. **207**, 62-75.

Yuan, W., Zhou, L., Chen, J. H., Wu, J. Y., Rao, Y. and Ornitz, D. M. (1999b). The mouse SLIT family: secreted ligands for ROBO expressed in patterns that suggest a role in morphogenesis and axon guidance. *Dev. Biol*. **212**, 290-306.